2,6-Di-tert-butylpyridine Sorption Approach to Quantify the External Acidity in Hierarchical Zeolites

ARTICLE *in* THE JOURNAL OF PHYSICAL CHEMISTRY C · MAY 2014

Impact Factor: 4.77 · DOI: 10.1021/jp501928k

3 AUTHORS:

Kinga Góra-Marek
Jagiellonian University
73 PUBLICATIONS **509** CITATIONS
SEE PROFILE

Karolina Tarach
Jagiellonian University
24 PUBLICATIONS **148** CITATIONS
SEE PROFILE

Minkee Choi
Korea Advanced Institute of Science and Tech…
45 PUBLICATIONS **3,224** CITATIONS
SEE PROFILE

THE JOURNAL OF PHYSICAL CHEMISTRY C

Article

pubs.acs.org/JPCC

2,6-Di-*tert*-butylpyridine Sorption Approach to Quantify the External Acidity in Hierarchical Zeolites

Kinga Góra-Marek,*[†] Karolina Tarach,[†] and Minkee Choi[‡]

[†]Faculty of Chemistry, Jagiellonian University in Kraków, Ingardena 3, 30-060 Krakow, Poland

[‡]Department of Chemical and Biomolecular Engineering, Korea Advanced Institute of Science and Technology, Daejeon 305-701, Republic of Korea

Supporting Information

ABSTRACT: This work was aimed to evidence that substituted pyridine, 2,6-di-*tert*-butylpyridine, is a suitable probe for the quantitative investigation of the external acidity in hierarchically structured zeolites. The 2,6-di-*tert*-butylpyridine was too large to enter the micropores, even in wide pore zeolites, and nearly no sites in nonmesoporous zeolites were available. Accessibility studies of acid sites in zeolites TNU-9 and BEA involving quantitative IR measurements with hindered 2,6-di-*tert*-butylpyridine as a probe were performed. The extinction coefficients of the 1615 cm^{-1} diagnostic bands of 2,6-di-*tert*-butylpyridine interacting with Brønsted acid sites were determined. Lewis acid sites were not detected with the probe. The accessibility factor (AF) for the 2,6-di-*tert*-butylpyridine probe molecule was defined as the number of sites detected by adsorption of the dTBPy (external sites) divided by the total amount of acid sites in the studied zeolites as quantified by pyridine sorption. Upon desilication resulting in the fabrication of the secondary mesopores, the enhanced accessibility of the protonic sites was observed. In comparison to the mesoporous zeolites with the secondary system of mesopores generated by alkaline leaching, considerably higher accessibility of protonic sites was evidenced in both ultrathin ZSM-5 and delaminated ITQ-2 zeolite.

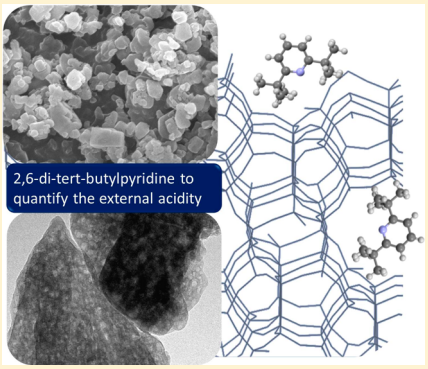

1. INTRODUCTION

Distinctive properties of zeolites, e.g., a well-defined micropore system and the presence of the acid sites of high strength, are the most important features responsible for an application of these materials as catalysts. However, their catalytic efficiency is restricted by diffusional limitations, which can induce a poor catalytic performance reflecting it as poor selectivity and short catalyst lifetime.[1,2] To improve the catalyst effectiveness, several top-down[3,4] and bottom-up[5,6] approaches of obtaining hierarchical zeolites with secondary mesoporosity have been proposed. The generation of secondary mesoporosity in zeolites can significantly shorten the diffusion path length[7] and hence improves the reactant transport to and from active sites. Various synthesis methods such as desilication,[8,9] delamination,[10,11] and supramolecular templating[12,13] (ultrathin ZSM-5) have been reported, but so far most of the works have focused on the synthesis and analysis of pore structure of the materials. It should be noted that catalytic functions of zeolites are determined not only by the pore structural properties but also by the spatial distribution of the acid sites. Desilication of zeolites by their leaching in alkaline solutions has appeared as the most effective, adjustable, and economic method for the hierarchical zeolites engineering. Since pioneering papers of Groen et al.,[8,9] a lot of effort has been devoted to the optimization of the desilication conditions and the elucidation of the desilication mechanism, especially to the realumination process on the mesopore surface, which has been found as an important factor in acidity modification. In addition to the concentration and strength of acid sites, their spatial distribution is the important factor determining the catalytic application of hierarchical zeolites. The first attempts to discriminate between the external and internal acid sites have been made by Busca and co-workers.[14] A series of branched nitriles have been selected to estimate the number of acid sites hidden in micropores and exposed on mesopores or the external surface of crystals. From the drop of the Si(OH)Al group band intensity, caused by the sorption of a bulky molecule, the number of external sites has been estimated. Another method has proposed the coadsorption of a small molecule (e.g., CO) and a hindered one (e.g., pivalonitrile, lutidine, collidine). This approach used the determination of the total number of sites by small molecule adsorption after poisoning of the external sites with a hindered base. Thus, the CO coadsorption can reveal the sites inaccessible for the bulky molecule. Thibault-Starzyk et al.[15,16] also reported the IR spectroscopy of substituted pyridines with different kinetic diameter (pyridine: 0.54 nm, lutidine: 0.67 nm, and collidine: 0.74 nm) and basic strength as a simple and powerful methodology to quantify the enhanced accessibility of acid sites in hierarchically structured zeolites. However, it should be

Received: February 24, 2014
Revised: April 2, 2014
Published: May 20, 2014

   dx.doi.org/10.1021/jp501928k | *J. Phys. Chem. C* 2014, 118, 12266−12274

noted that these two methods are not free of difficulties. First, in some cases the band of the Si−OH−Al groups (3300−3800 cm^{-1}) cannot be evaluated as it is covered either by the bands of the silanols groups bonded to the probes or by the bands of the probes themselves (such as pyridine, lutidine, and collidine). Moreover, for some structures, such as aluminosilicates, the Si−OH−Al groups' band has been hardly detected.[17,18] Consequently, the intensities of the Si−OH−Al bands free or engaged in interaction with CO or other probes (CO or others) cannot be measured accurately.

The first method of a quantitative investigation of the accessibility of both Brønsted and Lewis acid sites in hierarchical zeolites has been carried out by using IR studies of pivalonitrile adsorption.[19] The extinction coefficients of the diagnostic bands of pivalonitrile interacting with the acid sites of both kinds have been determined, and consequently, the concentration of sites accessible to pivalonitrile has been calculated. Nevertheless, it has been evidenced that at higher temperature thermal vibrations of the zeolite framework make the structure more flexible, and the pivalonitrile molecules could penetrate even the 10 MR channels of zeolite ZSM-5. Therefore, to quantify the accessibility of the sites in hierarchically structured zeolites, the molecule with significantly larger kinetic diameter is strongly required.

This work is attempted to evidence that substituted pyridine, 2,6-di-*tert*-butylpyridine, is a suitable probe for quantitative investigation of the external acidity in hierarchically structured zeolites that are synthesized by using different strategies and possess different crystalline (microporous) structures. The 2,6-di-*tert*-butylpyridine is too large to enter the micropores, even in wide pore zeolites (1.05 nm), and reaches nearly no sites in the solely microporous zeolites. Finally, the 2,6-di-*tert*-butylpyridine was used to differentiate between the overall concentration of acid sites and those mainly located on the external surface of parent and modified zeolites. Upon the fabrication of mesopores, the enhanced accessibility of the bulky molecules related to exposed external sites is believed to be selectively detectable by hindered 2,6-di-*tert*-butylpyridine. It should be noted that for the calculation of the concentration of acid sites accessible to 2,6-di-*tert*-butylpyridine the value of the extinction coefficient typical of pyridinium ions PyH^+ has been occasionally applied, however, offering the semiquantitative approach only.[20−22] Therefore, the determination of the extinction coefficient of $dTBPyH^+$ ions seems to be the most demanded task.

2. EXPERIMENTAL SECTION

Parent BEA zeolite of Si/Al = 22 was supplied by Zeolyst (CP 814C). Zeolite TNU-9 was synthesized according to a published procedure given in ref 23. Desilication was carried out in the 0.2 M solutions of NaOH and NaOH and TBAOH (tetrabutylammonium hydroxide) mixture (TBAOH/(NaOH + TBAOH) = 0.4) at the temperature of 338 K for 30 min. The 100 mL of solution was added to 3.0 g of zeolite. After desilication the suspension was cooled in an ice-bath, filtered, and washed until neutral pH. Next, a 4-fold ion-exchange with 0.5 M NH_4NO_3 was performed at 330 K for 1 h. Finally, the zeolites were again filtrated, washed with distillate water, and dried overnight at room temperature.

The samples of MCM-22 of Si/Al = 50 and its delaminated derivative ITQ-2 obtained from the same precursor were synthesized in the Instituto de Tecnología Química (ITQ), Universitat Politècnica de València (UPV).

ZSM-5 of Si/Al = 36 and its ultrathin analogue (hereafter denoted as AS-8) have been synthesized according to the procedure given in the literature.[24]

The amorphous mesoporous aluminosilicates HAlMCM-41,[25] HAlMCM-48,[26] both of Si/Al = 10, as well as sponge-like mesoporous aluminosilicates,[27] SA-2 (Si/Al = 2), SA-5 (Si/Al = 5), and SA-10 (Si/Al = 10), were synthesized as reported elsewhere and used as the calibration materials for determining the extinction coefficient of 2,6-di-*tert*-butylpyridine (hereafter denoted dTBPy). XRD, TEM, and BET experiments showed that the pore system of all the above-mentioned mesoporous aluminosilicates has been preserved upon the pretreatment to 900 K.

Prior to FTIR studies, all studied materials were pressed into the form of self-supporting discs (ca. 5−10 mg/cm^2) and pretreated in situ in an IR cell at 773 K under vacuum conditions for 1 h. Spectra were recorded with a Bruker Tensor 27 spectrometer equipped with an MCT detector. The spectral resolution was 2 cm^{-1}. All the spectra presented in this work were normalized to 10 mg of sample.

The total concentration of the Brønsted acid sites in calibration materials was determined in quantitative IR studies of pyridine sorption according to the procedure described in refs 17 and 18. Pyridine was supplied by Sigma-Aldrich (≥99.8%).

The excess of 2,6-di-*tert*-butylpyridine (hereafter denoted dTBPy), supplied by Sigma-Aldrich (≥97%), was adsorbed at 473 K, and then physisorbed molecules were subsequently removed by evacuation at the same temperature.

Si and Al concentrations in the parent and desilicated zeolites were determined by the ICP OES method with the Optima 2100DV (PerkinElmer) spectrometer.

The N_2 sorption processes at 77 K were studied on an ASAP 2420 Micromeritics after activation in vacuum at 670 K for 12 h. The *t*-plot method with the Harkins−Jura reference isotherm was used to determine the micropore volume (V_{micro}) and the external surface area (S_{meso}). Pore size distribution and volume of mesopores (V_{meso}) were obtained by the BJH model following the adsorption branch of the isotherm.

The powder X-ray diffraction (XRD) measurements were carried out using a PANalytical Cubix diffractometer, with Cu Kα radiation, λ = 1.5418 Å, and a graphite monochromator in the 2θ angle range of 2−40°. X-ray powder patterns were applied for structural identification of the relative crystallinity value (% Cryst) for all the zeolites. The determination of the relative crystallinity value was based on the intensity of the characteristic peaks in the range between 20.0° and 24.0° for BEA zeolites and 21.0° and 26.0° for TNU-9 zeolites.

3. RESULTS AND DISCUSSION

3.1. Sorption of Pyridine in Calibration Materials. The quantitative approach presented in this work is based on the nature of acid sites in aluminosilicates selected as the calibration materials. Thus, the acidic properties of the aluminosilicates, determined in quantitative experiments of pyridine sorption, will now be discussed.

The concentrations of Brønsted acid sites in sponge-like aluminosilicates SA(X),[27] detected by pyridine as a probe, increase with the Si content. Besides, the B/Al values, expressed as the ratios of the concentration of Brønsted sites and the total amount of Al in aluminosilicates, also increase with Si/Al. The increase of the fraction of aluminum atoms able to form Brønsted sites (Table 1) is related to the enhancement of the

dx.doi.org/10.1021/jp501928k | J. Phys. Chem. C 2014, 118, 12266−12274

Table 1. Mesopore Surface Area and the Concentration of Brønsted and Lewis Acid Sites in Calibration Materials Measured in the Quantitative Experiments of Pyridine Sorption[a]

			concentration of sites [μmol g^{-1}]		
zeolite	Si/Al	S_{BET} [m^2 g^{-1}]	Brønsted	Lewis	B/Al[a]
SA-2	2	540	200	450	0.03
SA-5	5	750	230	460	0.09
SA-10	10	1220	400	210	0.22
HAlMCM-48	10	1190	750	400	0.42
HAlMCM-41	10	1250	340	240	0.19

[a]The concentration of Brønsted sites per 1 Al atom (B/Al).

surface area, thus more Al atoms are exposed on the surface and can participate in the formation of Brønsted sites.[27] The concentration of Lewis sites decreases with Si content due to the transformation of surface Al species, i.e. potential Lewis sites, into the Si(OH)Al groups and also to dilution of the aluminosilicate material with Si species.

Different synthesis conditions, e.g., temperature, chemicals used, and synthesis procedure, can influence the extent of Al incorporation and/or its distribution within the mesoporous structure, and finally they can affect the acidic properties of the resulting aluminosilicates. It is well seen when comparing the aluminosilicates of the same Si/Al ratio but various structures: SA(10),[27] HAlMCM-41,[25] and HAlMCM-48[26] (Table 1). The HAlMCM-41[25] and SA(10)[27] were carried out by the template route, but with the various cationic surfactants. Finally, SA(10) possesses no order in the pore arrangement (disordered hexagonal or sponge-like pore distribution), whereas typical hexagonal structure was confirmed for HAlMCM-41 material. A mesoporous aluminosilicate molecular sieve of HAlMCM-48 type was prepared by grafting aluminum onto a purely siliceous material. Both the concentrations of Brønsted acid sites as well as the B/Al value are the highest in the case of HAlMCM-48, evidencing that the grafting of Al in MCM-48 is the most effective method to generate a large amount of Brønsted acid sites in amorphous aluminosilicates.

3.1. Determination of the Extinction Coefficients of IR Bands of 2,6-Di-*tert*-butylpyridine Interacting with Brønsted and Lewis Acid Sites. The key problem in IR quantitative studies is determination of the extinction coefficients of all the diagnostic bands. The main requirement is to elaborate the experimental conditions in which the probe molecule reacts selectively with acid species according to known stoichiometry. The simplest and the most desired is the situation when each molecule introduced into the IR cell reacts selectively with only one kind of adsorption site. The sorption of the 2,6-di-*tert*-butylpyridine (dTBPy) perfectly obeys this requirement. The IR spectra of the dTBPy adsorbed on the studied materials are shown in Figure 1.

To identify the diagnostic bands of dTBPy interacting with both Brønsted and Lewis acid sites, the sorption of the probe has been carried out on zeolites possessing a significant amount of acidic sites exposed on external surfaces: delaminated zeolite ITQ-2 (Figure 1, spectrum a). Interaction of the dTBPy with acid sites in zeolite ITQ-2 containing Brønsted acid sites as principal species (Brønsted and Lewis acid sites, 310 and 20 μmol g^{-1}, respectively) results in the decrease of the Si−OH−Al band (3620 cm^{-1}) (Figure 2) and the appearance of the 1615 cm^{-1} dTBPyH$^+$ band attributed to the dTBPy bonded to

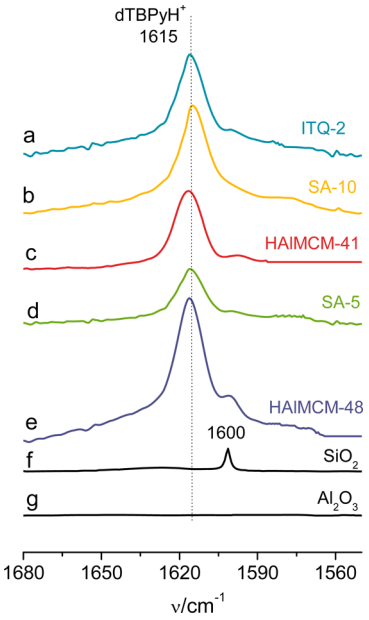

Figure 1. IR spectra of 2,6-di-*tert*-butylpyridine (dTBPy) adsorbed on the calibration materials.

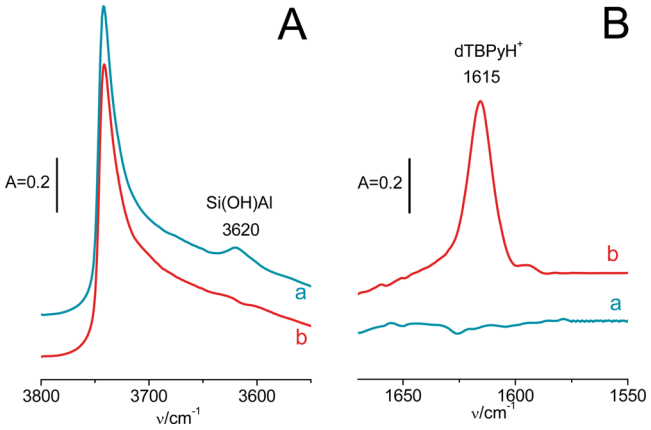

Figure 2. Spectra of OH groups (A) and of adsorbed 2,6-di-*tert*-butylpyridine (dTBPy) (B) on ITQ-2 zeolite. Spectra a were recorded before and spectra b after dTBPy adsorption.

Brønsted sites (Figure 1, spectrum a). It evidences that some Si−OH−Al groups in ITQ-2 are reached by the dTBPy molecules. The dTBPy sorption in mesoporous aluminosilicates HAlMCM-41, HAlMCM-48, SA-5, and SA-10, holding exclusively the acid sites exposed on the mesopore surface, also results in the appearance of the 1615 cm^{-1} dTBPyH$^+$ band (spectra b−e). The 1600 cm^{-1} band of slight intensity, typical of the spectra of all studied aluminosilicates, results from the interaction of dTBPy with Si−OH groups (spectrum f). It should be mentioned that Corma et al. in a very elegant manner[28] exhibited that also the 3370 cm^{-1} band of the ≡N−H$^+$ stretching vibration of protonated DTBPy could be used as adequate for characterizing Brønsted sites.

The spectra of dTBPy sorbed in aluminosilicates do not reveal the presence of the bands at 1600−1590 and 1450 cm^{-1} which may be attributed to the dTBPy coordinatively bonded to Lewis acid sites (dTBPy-L) regardless of their presence in studied aluminosilicates in huge quantity (Table 1). The same can be concluded from the analysis of spectra of dTBPy

dx.doi.org/10.1021/jp501928k | J. Phys. Chem. C 2014, 118, 12266−12274

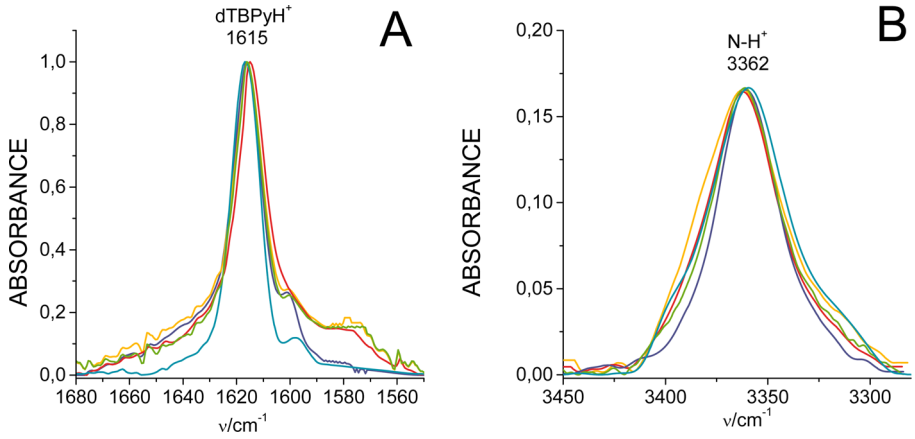

Figure 3. Spectra of dTBPy adsorbed on calibration materials normalized to the same intensity of the 1615 cm^{-1} $dTBPyH^+$ band (A) and the same spectra presented in the region of N−H vibration.

adsorbed on mesoporous Al_2O_3, and no bands of dTBPy interacting with electron acceptor sites are detected (spectrum g). What is more, in the region of the N−H stretching vibrations the 3650 cm^{-1} band of the ≡N−H^+ of protonated dTBPy is the only band, and it is not affected by the presence of others sites, i.e., Lewis acid sites. Additionally, the spectra of dTBPy adsorbed on calibration materials normalized to the same intensity of the 1615 cm^{-1} band are shown (Figure 3A). In these normalized spectra, the 3650 cm^{-1} bands of the ≡N−H^+ of protonated dTBPy (Figure 3B) are also of the same intensity for all studied materials, evidencing that both bands originated from the same moiety. Finally, it can be concluded that the 2,6-di-*tert*-butylpyridine can be considered to be selective for Brønsted sites because it is able to be protonated by Brønsted acid sites, and steric constraints prevented its coordination to Lewis sites via nitrogen lone electron pairs.[28−33]

Thus, in this work the possibility of the bonding of dTBPy to electron acceptor Lewis sites in zeolites and aluminosilicates has been excluded. Consequently, the presented approach of the quantitative procedure has concerned the concentration of Brønsted acid sites only.

The presented method includes three stages. At the first stage wide pore structures have been selected as calibration materials (HAlMCM-41, HAlMCM-48, SA-2, SA-5, and SA-10). These structures ensure the same number of sites detected by adsorption of pyridine and its substituted derivative, dTBPy. Second, for all calibration materials the total concentration of acid sites has been determined in quantitative experiments of pyridine sorption. Since that, the number of acid sites which could be detected by dTBPy has been perfectly known. The final step of the experimental part was the sorption of the dTBPy at 473 K, in an amount sufficient to saturate all accessible Brønsted acid sites, the evacuation of the physisorbed molecules, and finally, the determination of the maximum intensities of the diagnostic $dTBPyH^+$ band at 1615 cm^{-1} originated from the interaction of dTBPy with protonic sites in the calibration mesoporous aluminosilicates. All calibration materials used for this purpose are listed in Table 1. The difference in the structure types, the presence of mesopore systems of different architecture, and the various concentrations of protonic sites defined by the variety of Si/Al ratio allowed us to establish the value of the extinction coefficient independent of the type of the mesoporous material.

The maximum intensity of the 1615 cm^{-1} band (Figure 4A) as well as its integral intensity (Figure 4B), measured for all

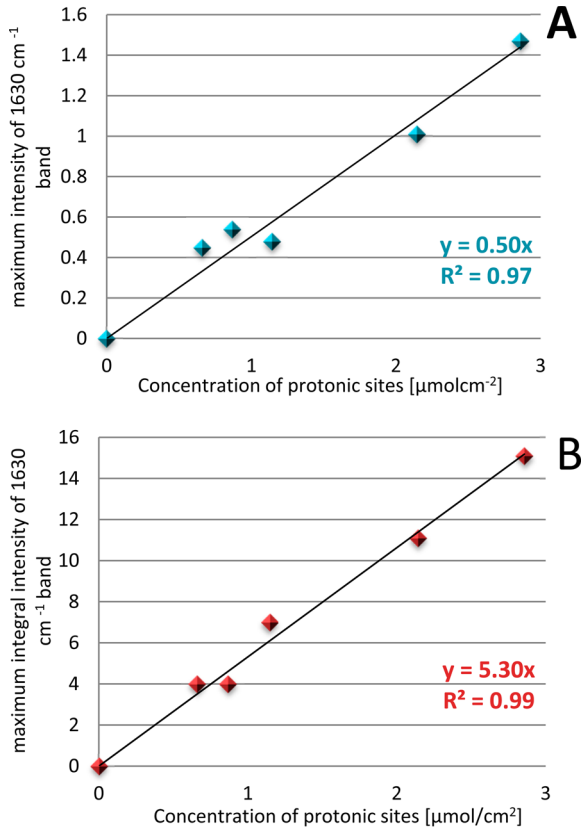

Figure 4. Plots of the calibration lines, based on the height (A) or the area (B) of the 1630 cm^{-1} $dTBPyH^+$ ion's band, applied for the determination of the Brønsted acid sites concentration.

calibration materials, were plotted as a function of overall concentration of the protonic sites, obtained previously in quantitative experiments of pyridine sorption. For all studied materials the linear dependence was obtained. Values of the extinction coefficients found as the slope of this line were equal to 0.5 and 5.3 cm^2 μmol^{-1}, respectively. For all the calibration materials all the experimental points fit the same line, regardless of their structure, acidity, and the different mesopore architectures. Consequently, the extinction coefficient of the

dx.doi.org/10.1021/jp501928k | J. Phys. Chem. C 2014, 118, 12266−12274

$dTBPyH^+$ ion band can be applied for the investigation of the accessibility of Brønsted acid sites in zeolites and mesoporous aluminosilicates of various structure and acidity. It should be also noted that the values of the extinction coefficients of the bands of pyridine bonded to Brønsted acid sites at ca. 1545 cm^{-1} (ε = 0.06 cm^2 μmol^{-1}) have been reported to be independent of the type of zeolite or mesoporous aluminosilicates.[34,35]

The values of extinction coefficients are governed by the change of dipole moment and consequently by the extent of charge separation within a molecule determined by its geometry. Values of the extinction coefficients found for the 1637 cm^{-1} bands for 2,4,6-trimethylpyridine[36] (collidine, Coll) and 2,6-di-*tert*-butylpyridine were equal to 0.62 and 0.50 cm^2 μmol^{-1}, respectively. As can be noticed they decrease with the number of atoms composing the probe molecule. The electron density is dissipated among all molecule's atoms; in consequence, for larger molecules the dipole moment is changed to a lesser extent. On the other hand, the extinction coefficients evaluated on the consecutive adsorption of the substituted alkylpyridines (2,4,6-trimethylpyridine (Me_3Py) and 2,4,6-triethylpyridine (Et_3Py)) by means of a McBain balance placed in an IR cell[36] have not revealed a similar trend. The extinction coefficients for dealuminated mordenites were the following: $\varepsilon(Me_3Py)$ = 10.1 cm μmol^{-1} and $\varepsilon(Et_3Py)$ = 10.5 cm μmol^{-1}.

3.3. Structural Characterization of Hierarchical Zeolites Synthesized Using Different Methods. Alkaline treatment leading to the preferential silicon extraction from the zeolite framework has been proven to be the effective way for engineering the mesoporosity in zeolites of the different types. Especially, the 10 MR and 12 MR zeolites of medium Si/Al ratio have been found to be the most suitable for desilication.[37] In this respect hierarchical zeolites BEA (12 MR) and TNU-9 (10 MR), used in these accessibility investigations, have been prepared by alkaline treatment. Pure NaOH (0.2 M) and a mixture of NaOH and TBAOH were used as desilicating agents. The presence of TBAOH in the desilicating mixture has been found to affect not only the chemical composition of the resulting materials but also the structure of the generated mesoporosity.[38] The last factor is responsible for substantial differences in the accessibility of protonic sites to hindered 2,6-di-*tert*-butylpyridine molecules (see Table 2).

The parent zeolite BEA was commercially available zeolite. Zeolite TNU-9 was synthesized according to a given procedure.[23] The XRD patterns confirmed fully crystalline character of both parent samples (Figure 1, Supporting Information). Micropore volumes of 0.18 and 0.17 cm^3 g^{-1} are typical of BEA and TUN structures, respectively (Table 2). Furthermore, the textural parameters derived from low-temperature nitrogen sorption demonstrated that both native zeolites BEA (S_{meso} = 44 m^2 g^{-1}) and TNU-9 (S_{meso} = 20 m^2 g^{-1}) possess limited mesoporosity attributed to the external surface of zeolite grains and surface roughness (Table 2). The BJH pore size distribution confirmed purely microporous character of both native samples (Figure 2, Supporting Information). Also the TEM micrograph showed no evidence for the presence of intracrystalline mesoporosity (Figure 3, Supporting Information).

The XRD patterns (Figure 1, Supporting Information) have shown that desilication of BEA zeolite with NaOH only led to considerable loss of crystallinity, while the treatment with NaOH and TBAOH allowed us to preserve zeolite structure. The fully crystalline character of NaOH- and TBAOH-treated BEA zeolite was confirmed by only a slight drop of the micropore volume (V_{micro} = 0.14 cm^3 g^{-1}). Contrarily, for material desilicated with NaOH the microporosity has been relatively reduced (S_{meso} = 510 m^2 g^{-1}; V_{micro} = 0.10 cm^3 g^{-1}) due to the formation of the amorphous phase (Table 2). Nevertheless, the alkaline treatment of zeolite BEA has resulted in the substantial development of mesopore surface area independently of desilicating agent (BEA/NaOH and TBAOH; S_{meso} = 468 m^2 g^{-1}). On the other hand, the desilication process of TNU-9 zeolites did not disturb the crystallinity of the resulting materials (Table 2), and the zeolite structure was fully preserved. The same conclusion can be drawn from the values of V_{micro}, which were not significantly affected by the development of a secondary system of mesopores. For desilicated zeolite TNU-9 no loss of microporosity has been observed. Both alkaline-treated zeolites are characterized by the same values of micropore volumes, while the mesopore surface area is significantly enhanced.

The TBAOH presence during alkaline treatment affects not only the crystallinity of the resulting zeolites but also the character of the created mesopore system. The BJH pore size distributions (Figure 2, Supporting Information) indicated that the TBAOH presence forces the generation of narrower and more uniform in diameter mesopores in comparison to materials treated with NaOH only, for both BEA and TNU-9 zeolites. This effect, however, is more profound for BEA zeolite than in the case of higher Al content TNU-9 zeolite. This can be elucidated by considering two aspects: (i) the role both of Al extracted from zeolite framework and tetrabutylammonium cation (TBA^+) as pore directing agents (PDA) and (ii) differences in pore structure and crystal morphology between studied zeolites. The first aspect has been already discussed in the literature[19,37] regarding also other organic cations such as PDA,[39] and it has been concluded that with increasing content of Al in the desilicating mixture, previously extracted from the zeolite framework, the formed mesopores exhibit wider pore size distribution and more superficial character. The second aspect associated with differences in pore size and crystal morphology between BEA and TNU-9 zeolites implies that the structure with 12 MR pores and grains with less regular shape and highly rough surface of BEA zeolite (well seen in TEM micrographs; Figure 3, Supporting Information), i.e., with a high amount of structural defects, favors the formation of mesopores in general. This effect is being reflected also by the formation of substantial amounts of narrower pores in the TBAOH presence. The IR quantitative studies of pyridine

Table 2. Physicochemical Properties of Studied Materials

zeolite	cryst. [%]	S_{BET} [m^2 g^{-1}]	S_{meso} [m^2 g^{-1}]	V_{micro} [cm^3 g^{-1}]
BEA/parent	100	567	44	0.18
BEA/NaOH	66	668	510	0.10
BEA/NaOH&TBAOH	100	793	468	0.14
TNU-9/parent	100	362	20	0.17
TNU-9/NaOH	96	450	103	0.17
TNU-9/NaOH&TBAOH	90	477	120	0.18
MCM-22[39]	-	451	96	0.18
ITQ-2[39]	-	841	796	0.02
ZSM-5	100	350	30	0.13
AS-8[24]	-	555	290	0.13

dx.doi.org/10.1021/jp501928k | J. Phys. Chem. C 2014, 118, 12266−12274

Table 3. Concentration of the Brønsted Acid Sites in Native and Desilicated Zeolites Measured in Quantitative Experiments of Pyridine (Py) and 2,6-Di-*tert*-butylpyridine (dTBPy) Sorption

			PyH^+ [μmol·g^{-1}]	$dTBPyH^+$ [μmol·g^{-1}]	accessibility factor
zeolite	Si/Al	Al [μmol g^{-1}]	Brønsted	Brønsted	$PyH^+/dTBPyH^+$
BEA/parent	22.1	675	395	10	0.03
BEA/NaOH	13.2	1100	450	120	0.27
BEA/NaOH&TBAOH	15.9	975	650	210	0.32
TNU-9/parent	14.6	990	850	10	0.01
TNU-9/NaOH	11.1	1290	930	130	0.14
TNU-9/NaOH&TBAOH	11.5	1240	1045	220	0.21

Table 4. Concentration of the Brønsted Acid Sites in Native and Modified Zeolites Measured in Quantitative Experiments of Pyridine (Py) and 2,6-Di-*tert*-butylpyridine (dTBPy) Sorption

			PyH^+ [μmol·g^{-1}]	$dTBPyH^+$ [μmol·g^{-1}]	accessibility factor
zeolite	Si/Al	Al [μmol·g^{-1}]	Brønsted	Brønsted	$PyH^+/dTBPyH^+$
MCM-22	50	330	300	10	0.03
ITQ-2	50	330	310	230	0.65
ZSM-5	36	410	345	15	0.04
AS-8[24]	36	410	400	180	0.50

adsorption have verified an increase of the protonic site concentration as a result of the decrease of Si/Al (Table 3).

The ultrathin zeolite ZSM-5 (Si/Al = 36) was synthesized using gemini-type quaternary ammonium surfactants as a structure-directing agent (SDA). The resultant material (AS-8) exhibited a typical XRD pattern for an MFI structure.[20] The ultrathin zeolite is built with the random assembly of "flake-like" zeolite crystals, and this morphology resulted from the zeolite crystals that were anisotropically grown to form a 2-dimensional sheet-like structure with 2−6 nm thickness.[24] The values of external surface areas clearly show that ultrathin zeolite AS-8 (290 m^2 g^{-1}) samples possess much larger external surface area than bulk ZSM-5 (30 m^2 g^{-1}). Both zeolites ZSM-5 (bulk and ultrathin) possess similar micropore volume (0.13 cm^3 g^{-1}), which corresponded to a micropore volume of zeolite ZSM-5.

Delaminated ITQ-2 zeolite is characterized by a remarkably large accessible external surface area (ca. 800 m^2 g^{-1}) and reduced microporosity (0.02 cm^{-3} g^{-1}) in comparison to its precursor MCM-22 (external surface area ca. 100 m^2 g^{-1} and microporosity (0.18 cm^3 g^{-1})) (Table 2).

3.4. Concentration of Acid Sites Accessible to 2,6-Di-*tert*-butylpyridine. A newly developed approach has been used to differentiate between the overall concentration of acid sites and those located on the external surface of hierarchical zeolites obtained by desilication (TNU-9, BEA; see Table 2), delamination (ITQ-2; see Table 3), and direct synthesis with gemini-type quaternary ammonium surfactant (AS-8; see Table 3) and their microporous analogues. In general, all those approaches lead to the development of external surface area, thus shortening the diffusion pathway for adsorbed molecules. The external surface area can also refer to the crystal size, thus the direct comparison of accessibility of acid sites should be performed with respect to the changes of the crystal size as was evidenced in the work of Corma and co-workers.[28]

The dTBPy was adsorbed on the zeolites at 473 K followed by evacuation at the same temperature to remove the excess of physisorbed probe molecules. The concentration of the protonic sites detected by the dTBPy was calculated from the maximum intensities of the $dTBPyH^+$ bands at 1625 cm^{-1} and its extinction coefficient, determined as described in Section 3.1. The accessibility factor (AF) for the 2,6-di-*tert*-butylpyridine probe molecule was defined as the number of sites detected by adsorption of the dTBPy (external sites) divided by the total amount of acid sites in the studied zeolites as quantified by pyridine sorption. The values of the accessibility factor (AF) are also presented in Tables 3 and 4.

Both the origin and concentration of Lewis acid sites are not discussed in this paper as the possibility of the bonding of dTBPy to electron acceptor Lewis sites in zeolites and aluminosilicates has been excluded (see Section 3.1).

3.4.1. Accessibility of Brønsted Sites in Desilicated Zeolites BEA and TNU-9. Figure 5 presents the AF values in the correlation with the mesopore surface in studied zeolites BEA and TUN. The negligible values of AFs for both native zeolites (0.02 for BEA and 0.01 for TNU-9) clearly evidence that accessibility of the Si(OH)Al groups for 2,6-di-*tert*-butylpyridine is sterically restricted (Table 3 and Figure 5). The 2,6-di-*tert*-butylpyridine is proved to be too large to enter the micropores in the native zeolites, even in the wide pore of zeolite BEA, and reaches nearly no sites. Upon the fabrication of mesopores, the enhanced accessibility of the bulky molecules related to exposed external sites is believed to be selectively

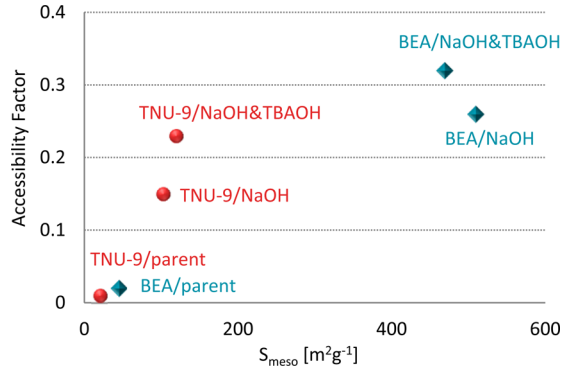

Figure 5. Plots of accessibility factor (AF) for protonic sites versus the surface of mesopores in parent zeolites and zeolites desilicated with NaOH and NaOH and TBAOH (TNU-9, red points; BEA, blue points).

dx.doi.org/10.1021/jp501928k | J. Phys. Chem. C 2014, 118, 12266−12274

detected by hindered 2,6-di-*tert*-butylpyridine. Upon desilication resulting in the fabrication of the secondary system of mesopores, the enhanced accessibility of the protonic sites is observed (Table 3 and Figure 5). The accessibility factors for Brønsted sites increases with mesopore surface. The increase of accessibility of the Brønsted acid sites to dTBPy molecules in alkaline-leached zeolites is associated with the increase of contribution of the sites located on external surfaces and in the zeolite pore mouths of high mesopore surfaces. The extended mesopore system and decreased average length of micropores in hierarchical zeolites in comparison to their native analogues are the decisive factor determining the accessibility of protonic sites. For both zeolites TNU-9 and BEA the Brønsted site accessibility is better for zeolites desilicated with NaOH and TBAOH mixture than with pure NaOH (Table 3) which is related to the development of the mesopore surface as a consequence of the formation of narrower diameter pores in the presence of TBA^+ as a pore-directing agent (Figure 5). What is more, the desilication was found to be more effective for zeolite BEA than zeolite TNU-9 since it is verified that the number of silicon atoms that could be removed with crystallinity preservation is governed by the framework topology and the type of desilicating agent used (see Section 3.3).

The enhancement of protonic site accessibility with the increasing external area in desilicated zeolites has been also reported for lutidine and collidine.[40] Moreover, the first method of a quantitative investigation of the accessibility in hierarchical zeolites has been based on quantitative IR studies of pivalonitrile adsorption.[19] Nevertheless, it has been evidenced that at higher temperature thermal vibrations of zeolite framework make the structure more flexible, and the pivalonitrile and collidine molecules, used for accessibility studies, were able to penetrate even the channels of zeolites ZSM-5[19] and BEA.[36,41] This has been confirmed by the total accessibility of sites (AF = 1) for pivalonitrile molecules in desilicated zeolites ZSM-5.[19] In the present work the total accessibility of protonic sites has been confirmed neither for zeolite BEA nor zeolite TNU-9, and the maximum number of external sites reaches 0.32 and 0.23, respectively. It evidences that the dTBPy molecule is suitable to quantify the accessibility of the sites in hierarchically structured zeolites.

3.4.2. Accessibility of Brønsted Sites in Zeolites: Delaminated ITQ-2 and Ultrathin ZSM-5. The concentration of protonic sites located on the external surface of hierarchical zeolites obtained by desilication (TNU-9, BEA; see Table 3) reached 32% of the overall concentration of acid sites. It was interesting to find out if this new approach could validate a greater accessibility to hindered molecules expected for the class of ultrathin and nanocrystalline zeolites that combines a large, catalytically active external surface. Therefore, the procedure of the quantitative dTBPy adsorption has been adapted for the accessibility investigations of Brønsted acid sites in zeolites with porosity within the layers. Zeolite ITQ-2, a delaminated precursor of zeolite MCM-22, is formed by single layers.[10] These layers consist of the external 12 MR cups and a 10 MR channel system running across the sheet and linking the cups. Ultrathin zeolite ZSM-5 of unit cell composition $H_{2.6}[(SiO_2)_{93.4}(AlO_2)_{2.6}]$, denoted as AS-8, has been synthesized with gemini-type quaternary ammonium surfactant, according to a procedure given in ref 24. The TEM image evidences that the ultrathin zeolite's material (AS-8) was built with a 2-dimensional sheet-like structure with 2−6 nm thickness.[24] The AF values calculated for both nanosheet morphology structures have been found to be even 3-fold higher than for desilicated zeolites (Table 4, Figure 6). It points

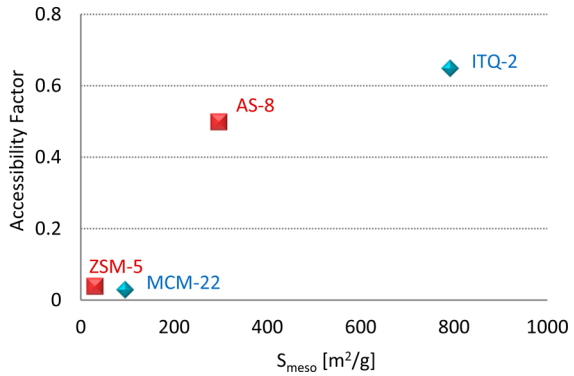

Figure 6. Plots of accessibility factor (AF) for protonic sites versus the surface of mesopores for zeolites ZSM-5 and MCM-22 and their analogues (ZSM-5, red points; MCM-22, blue points).

to a considerably higher accessibility of protonic sites in both delaminated and nanocrystalline zeolite in comparison to the materials with the secondary system of mesopores generated by alkaline leaching. Figure 6 presents the AF values in correlation with the mesopore surface in microporous conventional ZSM-5 and MCM-22 zeolites and their analogues. It is worth mentioning that for delaminated ITQ-2 the accessibility to dTBPy has been evidenced to be better than for ultrathin zeolite ZSM-5 (AS-8). The result shows that protonic sites contained within thin sheets of zeolite ITQ-2 are readily accessible due to noticeably higher mesopore surface area. Possibly, 2-dimensional sheet-like structure, assuring the higher contribution of external sites, is more effectively generated for ITQ-2.

4. CONCLUSIONS

In this work, it has been evidenced that substituted pyridine 2,6-di-*tert*-butylpyridine was a suitable probe for the quantification of the external protonic sites in parent and mesostructured zeolites. The experimental conditions of the quantitative procedure were elaborated, and the value of the extinction coefficient of the 1615 cm^{-1} $dTBPyH^+$ band was determined. Finally, 2,6-di-*tert*-butylpyridine was used to differentiate between the overall concentration of acid sites and those mainly located on the external surface of parent and modified zeolites. The concentration of protonic sites located on the external surface of desilicated zeolites (TNU-9, BEA) reached 32% of the overall concentration of acid sites, while a greater accessibility to 2,6-di-*tert*-butylpyridine molecules (65%) was validated for the class of ultrathin zeolites.

■ ASSOCIATED CONTENT

Supporting Information

The XRD diffraction patterns of studied zeolites (Figure 1). The BJH pore size distribution of studied materials (Figure 2). TEM micrographs of studied zeolites (Figure 3). This material is available free of charge via the Internet at http://pubs.acs.org.

AUTHOR INFORMATION

Corresponding Author

*Phone: +48 (12) 663-20-81. Fax: +48 (12) 634-05-15. E-mail: kinga.goramarek@gmail.com.

Author Contributions

The manuscript was written through contributions of all authors. All authors have given approval to the final version of the manuscript

Notes

The authors declare no competing financial interest.

ACKNOWLEDGMENTS

This work was financed by Grant No. 2013/09/B/ST5/00066 from the National Science Centre, Poland. The samples of zeolites MCM-22, ITQ-2, and TNU-9 were kindly supplied by Professor Avelino Corma and Susana Valencia from the Instituto de Tecnología Química (ITQ), Universitat Politècnica de València (UPV).

REFERENCES

(1) van Donk, S.; Janssen, A. H.; Bitter, J. H.; de Jong, K. P. Generation, Characterization, and Impact of Mesopores in Zeolite Catalyst. *Catal. Rev.: Sci. Eng.* **2003**, *45*, 297−319.

(2) Pérez-Ramírez, J.; Christensen, C. H.; Egeblad, E.; Christensen, C. H.; Groen, J. C. Hierarchical Zeolites: Enhanced Utilization of Microporous Crystals in Catalysis by Advances in Materials Design. *Chem. Soc. Rev.* **2008**, *37*, 2530−2542.

(3) van Donk, S.; Janssen, A. H.; Bitter, J. H.; de Jong, K. P. Generation, characterization, and impact of mesopores in zeolite catalysts. *Catal. Rev. Sci. Eng.* **2003**, *45*, 297−319.

(4) Pavel, C. C.; Palkovits, R.; Schüth, F.; Schmidt, W. The benefit of mesopores in ETS-10 on the vapor-phase Beckmann rearrangement of cyclohexanone oxime. *J. Catal.* **2008**, *254*, 84−90.

(5) Tosheva, L.; Valtchev, V. P. Nanozeolites: Synthesis, Crystallization Mechanism, and Applications. *Chem. Mater.* **2005**, *17*, 2494−2513.

(6) Egeblad, K.; Christensen, C. H.; Kustova, M. Y.; Christensen, C. H. Templating mesoporous zeolites. *Chem. Mater.* **2008**, *20*, 946−960.

(7) Chaikittisilp, W.; Suzuki, Y.; Mukti, R. R.; Suzuki, T.; Sugita, K.; Itabashi, K.; Shimojima, A.; Okubo, T. Formation of Hierarchically Organized Zeolites by Sequential Intergrowth. *Angew. Chem., Int. Ed.* **2013**, *52*, 3355−3359 and references therein.

(8) Groen, J. C.; Jansen, J. C.; Moulijn, J. A.; Pérez-Ramírez, J. Optimal Aluminum-Assisted Mesoporosity Development in MFI Zeolites by Desilication. *J. Phys. Chem. B* **2004**, *108*, 13062−13065.

(9) Groen, J. C.; Peffer, L. A. A.; Moulijn, J. A.; Pérez-Ramírez, J. Aldol Condensations over Reconstructed Mg-Al Hydrotalcites: Structure-Activity Relationships Related to the Rehydration Method. *Chem.−Eur. J.* **2005**, *11*, 4983−4994.

(10) Corma, A.; Fornés, V.; Pergher, S. B. C.; Maesen, T. L.; Buglass, J. G. Delaminated zeolite precursors as selective acidic catalysts. *Nature* **1998**, *396*, 353−356.

(11) Ogino, I.; Nigra, M. M.; Hwang, S.-J.; Ha, J.-M.; Rea, T.; Zones, S. I.; Katz, A. Delamination of Layered Zeolite Precursors under Mild Conditions: Synthesis of UCB-1 via Fluoride/Chloride Anion-Promoted Exfoliation. *J. Am. Chem. Soc.* **2011**, *133* (10), 3288−3291.

(12) Pal, N.; Bhaumik, A. Soft templating strategies for the synthesis of mesoporous materials: inorganic, organic-inorganic hybrid and purely organic solids. *Adv. Colloid Interface Sci.* **2013**, *189−190*, 21−41.

(13) Na, K.; Choi, M.; Ryoo, R. Recent advances in the synthesis of hierarchically nanoporous zeolites. *Microporous Mesoporous Mater.* **2013**, *166*, 3−19.

(14) Trobmetta, M.; Busca, G.; Lenarda, M.; Storaro, L.; Pavan, M. An Investigation of the Surface Acidity of Mesoporous Al-Containing MCM-41 and of the External Surface of Ferrierite through Pivalonitrile Adsorption. *Appl. Catal., A* **1999**, *182*, 225−235.

(15) Nesterenko, N. S.; Thibault-Starzyk, F.; Montouillout, V.; Youschnko, V. V.; Fernandez, C.; Gilson, J.-P.; Fajula, F.; Ivanova, I. I. Accessibility of the Acid Sites in Dealuminated Small-Port Mordenites Studied by FTIR of Co-Adsorbed Alkylpyridines and CO. *Microporous Mesoporous Mater.* **2004**, *71*, 157−166.

(16) Thibault-Starzyk, F.; Stan, I.; Abelló, S.; Bonilla, A.; Thomas, K.; Fernandez, C.; Gilson, J.-P.; Pérez-Ramírez, J. Quantification of Enhanced Acid Site Accessibility in Hierarchical Zeolites − the Accessibility Index. *J. Catal.* **2009**, *264*, 11−14.

(17) Góra-Marek, K.; Datka, J. IR Studies of OH Groups in Mesoporous Aluminosilicates. *Appl. Catal., A* **2006**, *302*, 104−109.

(18) Góra-Marek, K.; Derewiński, M.; Datka, J.; Sarv, P. IR and NMR Studies of Mesoporous Alumina and Related Aluminosilicates. *Catal. Today* **2005**, *101*, 131−138.

(19) Sadowska, K.; Góra-Marek, K.; Datka, J. Accessibility of Acid Sites in Hierarchical Zeolites: Quantitative IR Studies of Pivalonitrile Adsorption. *J. Phys. Chem. C* **2013**, *117*, 9237−9244.

(20) Jo, Ch.; Ryoo, R.; Žilková, N.; Vitvarová, D.; Čejka, J. The effect of MFI zeolite lamellar and related mesostructures on toluene disproportionation and alkylation. *Catal. Sci. Technol.* **2013**, *3*, 2119−2129.

(21) Kubů, M.; Roth, W. J.; Greer, H. F.; Zhou, W.; Morris, R. E.; Přech, J.; Čejka, J. A New Family of Two-Dimensional Zeolites Prepared from the Intermediate Layered Precursor IPC-3P Obtained during the Synthesis of TUN Zeolite. *Chem.−Eur. J.* **2013**, *19* (41), 13937−13945.

(22) Kubů, M.; Žilková, N.; Čejka, J. Post-synthesis modification of TUN zeolite: Textural, acidic and catalytic properties. *Catal. Today.* **2011**, *168* (1), 63−70.

(23) Hong, S. B.; Min, H. K.; Shin, Ch.H.; Cox, P. A.; Warrender, S. J.; Wright, P. A. Synthesis, crystal structure, characterization, and catalytic properties of TNU-9. *J. Am. Chem. Soc.* **2007**, *129*, 10870−10875.

(24) Kim, K.; Ryoo, R.; Jang, H.-D.; Choi, M. Spatial distribution, strength, and dealumination behavior of acid sites in nanocrystalline MFI zeolites and their catalytic consequences. *J. Catal.* **2012**, *288*, 115−123.

(25) Weglarski, J.; Datka, J.; He, H.; Klinowski, J. IR spectroscopic studies of the acidic properties of the mesoporous molecular sieve MCM-41. *J. Chem. Soc., Faraday Trans.* **1996**, *92*, 5161−5164.

(26) Rozwadowski, M.; Lezanska, M.; Wloch, J.; Erdmann, K. Al-MCM-48 as a template for synthesis of porous carbons - Adsorption study. *Stud. Surf. Sci. Catal.* **2007**, *158A*, 447−454.

(27) Góra-Marek, K.; Derewiński, M.; Datka, J.; Sarv, P. On the origin and nature of acid sites in mesoporous aluminosilicates. *Catal. Today* **2005**, *101*, 131−138.

(28) Corma, A.; Fornés, V.; Forni, L.; Marquez, F.; Martinez-Triguero, J.; Moscotti, D. 2,6-Di-tert-butyl-pyridine as a probe molecule to measure external acidity of zeolite. *J. Catal.* **1998**, *179*, 451.

(29) Baertsch, C. D.; Komala, K. T.; Chua, Y.-H.; Iglesia, E. Genesis of Brønsted Acid Sites during Dehydration of 2-Butanol on Tungsten Oxide Catalyst. *J. Catal.* **2002**, *205*, 44−57.

(30) Macht, J.; Baertsch, Ch.D.; May-Lozano, M.; Soled, S. L.; Wang, Y.; Iglesia, E. Support effects on Brønsted acid site densities and alcohol dehydration turnover rates on tungsten oxide domains. *J. Catal.* **2004**, *227*, 479−491.

(31) Liu, H.; Iglesia, E. Effects of support on bifunctional methanol oxidation pathways catalyzed by polyoxometallate Keggin clusters. *J. Catal.* **2004**, *223*, 161−169.

(32) Santiesteban, J. G.; Vartuli, J. C.; Han, S.; Bastian, R. D.; Chang, C. D. Influence of the preparative method on the activity of highly acidic WOx/ZrO2 and the relative acid activity compared with zeolites. *J. Catal.* **1997**, *168*, 431−441.

(33) Knozinger, H. Infrared Spectroscopy as a probe of surface acidity. In *Elementary Reaction Steps in Heterogeneous Catalysis*; Joyner, R. W., Santen, R. A., Eds.; NATO ASI Series; Springer: New York, 1993; Vol. *398*, pp 267−285.

(34) Datka, J. Transformations of but-1-ene molecules adsorbed in NaHY zeolites studied by infrared spectroscopy. *J. Chem. Soc., Faraday I* **1980**, *76*, 2437−2447.
(35) Sadowska, K.; Góra-Marek, K.; Datka, J. Hierarchical zeolites studied by IR spectroscopy: Acid properties of zeolite ZSM-5 desilicated with NaOH and NaOH/tetrabutylammonium hydroxide. *Vib. Spectrosc.* **2012**, *63*, 418−425.
(36) Mlekodaj, K.; Sadowska, K.; Datka, J.; Góra-Marek, K.; Makowski, W. Porosity and accessibility of acid sites in desilicated ZSM-5 zeolites studied using adsorption of probe molecules. *Microporous Mesoporous Mater.* **2014**, *183*, 54−61.
(37) Verboekend, D.; Perez-Ramirez, J. Design of hierarchical zeolite catalysts by desilication. *Catal. Sci. Technol.* **2011**, *1*, 879−890 and references therein.
(38) Peréz-Ramírez, J.; Verboekend, D.; Bonilla, A.; Abelló, S. Zeolite catalysts with tunable hierarchy factor by pore-growth moderators. *Adv. Funct. Mater.* **2009**, *19* (24), 3972−3979.
(39) Verboekend, D.; Vile, G.; Perez-Ramírez, J. Mesopore Formation in USY and Beta Zeolites by Base Leaching: Selection Criteria and Optimization of Pore-Directing Agents. *Cryst. Growth Des.* **2012**, *12*, 3123−3132.
(40) Nesterenko, N. S.; Thibault-Starzyk, F.; Montouilliout, V.; Yushchenko, V. V.; Fernandez, C.; Gilson, J.-P.; Fajula, F.; Ivanova, I. I. The use of the consecutive adsorption of pyridine bases and carbon monoxide in the IR spectroscopic study of the accessibility of acid sites in microporous/mesoporous materials. *Kinet. Catal.* **2006**, *47* (1), 40−48.
(41) Busca, G. Acid Catalysts in Industrial Hydrocarbon Chemistry. *Catal. Rev.: Sci. Eng.* **2007**, *107*, 5366−5410.